Composition Wheels: Visualizing dissolved organic matter using common composition metrics across a variety of Canadian Ecozones

Pieter J. K. Aukes[1,2¶*]

Sherry L. Schiff[1¶]

[1] Department of Earth & Environmental Studies, University of Waterloo, Waterloo, Ontario, Canada

[2] Geography & Environmental Studies, Wilfrid Laurier University, Waterloo, Ontario, Canada

* Corresponding author

E-mail: paukes@uwaterloo.ca (PJKA)

[¶]These authors contributed equally to this work.

Abstract

Dissolved organic matter (DOM) is a ubiquitous component of aquatic systems, impacting aquatic health and drinking water quality. These impacts depend on the mixture of organic molecules that comprise DOM. Changing climates are altering both the amount and character of DOM being transported from the terrestrial system into adjacent surface waters, yet DOM composition is not monitored as often as overall concentration. Many DOM characterization methods exist, confounding comparison of DOM composition across different studies. The objective of this research is to determine which parameters in a suite of relatively simple and common DOM characterization techniques explain the most variability in DOM composition from surface and subsurface sites. Further, we create a simple visualization tool to easily compare compositional differences in DOM. A large number of water samples (n=250) was analyzed from six Canadian ecozones for DOM concentration, ultraviolet-visible light absorbance, molecular size, and elemental ratios. Principal component analyses was used to identify quasi-independent DOM compositional parameters that explained the highest variability in the dataset: spectral slope, specific-UV absorbance at 255nm, humic substances fraction, and dissolved organic carbon to dissolved organic nitrogen ratio. A 'Composition Wheel' was created by plotting these four parameters as a polygon. Our results find similarities in DOM composition irrespective of site differences in vegetation and climate. Composition Wheels reveal two main shapes that correspond to common compositions of DOM regardless of site: DOM in the subsurface and DOM influenced by photodegradation The Composition Wheel approach uses easily visualized differences in polygon shape to quantify how DOM evolves by natural processes along the aquatic continuum and to track sources and degradation of DOM.

Introduction

Dissolved organic matter (DOM) is a pervasive component of aquatic environments and an important determinant of overall water quality and ecosystem function. For example, DOM dictates thermal and pH regimes within lakes [1], complexes with and mobilizes metals [2], and acts as an important redox constituent for biogeochemical reactions [3]. Further, DOM affects drinking water quality through taste, odour, and colour [4], consumption of added oxidizing chemicals, and reactions with chlorine during drinking water treatment processes to form carcinogenic disinfection by-products [5]. The overall reactivity of DOM is determined by its mixture of thousands of organic molecules with differing structural and chemical characteristics. Increased DOM concentrations in surface waters across the United Kingdom, Europe, and North America [1,6] and have been linked with declines to water transparency [1,7] and can have

significant effects upon future drinking water treatment options [8,9]. Yet, little information is found on the processes that dictate DOM composition and its impact on the surrounding environment [10]. Hence, quantifying changes to both the amount and composition of DOM across temporal and spatial scales allows for a better understanding of future changes to DOM and its influence upon water quality.

Both concentration and composition of DOM are used to identify the source, quality, and fate of DOM within the environment. The overall DOM concentration is operationally defined as the concentration of carbon in molecules passing through a chosen filter size (generally between 0.2 and 1.2 μm). Differences in DOM composition have been used to quantify hydrologic mixing and changes to redox potential [11]. Various options are available to characterize DOM, but many are expensive, analyze only a subfraction of the DOM, require complicated analysis, or are not widely accessible. For instance, Fourier-transform infrared spectroscopy (FTIR) analyses provides insightful and novel information on DOM composition [12,13] but is not readily available. Common compositional measures include ultraviolet or visible light absorbance [14–16], fluorescence [17,18], elemental ratios [19], and molecular weight and size [20]. Although absorbance parameters have been useful for tracking changes to DOM composition within riverine systems [16] and coastal wetlands [11], this method can be susceptible to interferences from the sample matrix, such as nitrate or iron [14,21]. However, corrections for such interference are dependent upon DOM quality, so correction algorithms are subject to circularity [22]. Thus, various characterization techniques can provide a holistic representation of the components that comprise DOM but are often sensitive to different components and interferences.

Dissolved organic matter is the net product of varying sources and degrees of processing at that point within the watershed. Quantifying changes to DOM composition along a hydrologic continuum can provide information on dominant sources or processes that influence DOM evolution [23]. Soil-derived aliphatic components of DOM are preferentially lost as water moves from subsurface to surface waters, at which point aromatic, high-nominal oxidation state DOM becomes further degraded along the fluvial network to more aliphatic, low nominal oxidation state DOM [12,24]. Increased degradation and processing of DOM along a system reduces its chemodiversity, with persistence of specific components linked to the original DOM composition [24–26]. Laboratory experiments have been used to isolate specific changes to DOM composition resulting from either microbial or photolytic degradation [27,28]. Hence, compositional measures can be used to better understand potential sources or processes that have resulted in the specific mixture of DOM at that point of sampling.

Recent progress in the understanding of DOM and carbon cycling has led to recognition of the importance of characterizing DOM composition along with concentration. Once in the aquatic system, differences in DOM properties and composition, or intrinsic controls, are thought to dictate DOM fate more-so than extrinsic controls such as temperature, nutrients, and sunlight exposure [24]. Recent modelling rates of microbial processing of DOM in surface waters include approaches that treat DOM as a heterogeneous mixture of compounds with varying decay rates, rather than a 0- or 1-order rate [29–31], allowing for specific DOM components to dictate overall degradation kinetics. Hence, DOM fate is closely linked to quantifying and comparing compositional changes over spatial and temporal scales.

Comparison of different DOM composition metrics have generally focussed on single hydrological environments (i.e. solely lakes [25] or rivers [32]) or on one or two measures across

spatial scales or varying environments. Given the complex mixture of organic compounds, and that different measures of DOM composition record different attributes, the combined use of several complimentary measures may provide a better characterization of DOM [28]. The objective of this study is to select the best suite of readily accessible DOM characterization techniques, create a simple, effective visual tool for comparison of DOM compositional differences, and assess the changes in DOM composition across environmental gradients. This objective will be accomplished in three parts: 1) determine which broadly-used measures of DOM composition capture the most variability within a dataset of surface and subsurface sites in various Canadian ecozones (groupings of similar areas of biodiversity [33]), 2) create a visualization tool to allow facile comparison of DOM from different samples based upon a set of quasi-independent composition measures, and 3) use the tool to explore differences in hydrological setting and climate across a range of northern environments.

Methods

Sites & sampling

Locations were selected where DOM was expected to differ due to differences in surrounding watershed characteristics (e.g. land use, wetland coverage, climate, and vegetation). Various surface and subsurface samples were collected from the Northwest Territories (Yellowknife, Wekweètì, Daring Lake), high arctic Nunavut (Lake Hazen Watershed), and Ontario (IISD-Experimental Lakes Area) (Fig 1; S1 Table). Surface water samples were collected 0.25 m below the surface from lakes, rivers, creeks, and ponds. Subsurface samples from northern locations (Yellowknife, Wekweètì, Daring Lake, Lake Hazen) were collected from the deepest extent of the mid-summer active-layer, just above the permafrost boundary (0.1 to

0.5 m below surface). Additional samples were collected from Turkey Lakes Watershed (ON), Nottawasaga River Watershed (ON), Grand River (ON), Mackenzie River (NT), and Black Brook Watershed (NB) to expand the ranges of individual composition measures but only overall DOM concentration and select composition metrics are available at these sites (Fig 1; S1 Table). A total of 250 samples were collected and analysed in this study.

Surface water samples were collected using a 60 mL syringe and filtered in-field using 0.45 μm syringe-tip filters (Whatman GD/X 45mm) into 40 mL acid-washed, pre-rinsed glass vials. Subsurface samples were collected using a peristaltic pump with an attached 0.45 μm syringe-tip filter. Vials and filters were pre-rinsed with filtered sample water before collection. Samples were kept cool (<4ºC) and in the dark until analysis at the University of Waterloo within three weeks of collection.

DOM quantity & composition analyses

Dissolved organic carbon and total nitrogen concentrations were measured using a Shimadzu Total Organic Carbon (TOC-L) Combustion Analyzer with TNM-1 module. Dissolved organic nitrogen (DON) was calculated as the difference between total dissolved nitrogen concentration and the sum of inorganic nitrogen species (nitrate, nitrite, and ammonium). Inorganic nitrogen species were measured using SmartChem 200 Automated Chemistry Analyzer (Unity Scientific, MA United States). The DOC:DON ratio was calculated using molar concentrations of DOC (M_C) and DON (M_N).

Absorbance was measured using a Cary 100 UV-VIS Spectrophotometer (Agilent, CA United States) at 5 nm increments from 200 to 800 nm. Deionized water was used to zero the instrument and run intermittently during analyses to correct for baseline drift. The Naperian absorption coefficient (a; m^{-1}) was calculated using:

$$a_\lambda = \frac{ln(10) \times A_\lambda}{L}$$

where A is the baseline-corrected absorbance at wavelength λ and L is the cell length (m). A suite of absorbance characteristics were then calculated (Table 1).

Molecular-size based fractions of DOM were determined using a size exclusion chromatography technique (Liquid Chromatography – Organic Carbon Detection, LC-OCD) at the University of Waterloo. Detailed instrument setup and analysis is described elsewhere [20]. Briefly, the sample was injected through a size-exclusion column (SEC; Toyopearl HW-50S, Tosoh Bioscience) that separated DOM based on hydrodynamic radii into five hydrophilic fractions (from largest to smallest): biopolymers (BP; polysaccharides or proteins), humic substances fraction (HSF; humic and fulvic acid fraction), building blocks (BB; lower weight humic substances), low molecular weight neutrals (LMWN; aldehydes, small organic materials), and LMW-acids (LMWA; saturated mono-protic acids). A portion of the sample by-passes the SEC for determination of the overall DOC concentration, here referred to as DOM concentration in mg C/L. A number average molecular weight was derived only for the HSF based on elution time. Duplicates run at six concentrations yield a precision for the LC-OCD of <0.1 mg C/L for all fractions. Concentrations of each fraction were calculated using specialized software (ChromCALC, DOC-Labor, Germany) that integrated chromatograms from the LC-OCD.

Statistical analyses & Composition Wheel design

Samples from sites with multiple sampling events were averaged to create a single value per site. Data were analysed using unconstrained ordination analysis via principal components analysis (PCA) on a subset of samples that contained all composition measures (subset n=130). Data were scaled before PCA and analysed using R Statistical Software [37].

The Composition Wheel (CW) is a polygon drawn from axes of various composition measures that are independent of DOM concentration in order to focus solely on differences in DOM composition. Composition Wheel parameters were chosen based on the highest contribution of variables explaining the first two principal component axes (S1 Fig). Further, independent measures of DOM composition were preferentially chosen to minimize overlap in information between similar techniques. Each CW axis corresponds to a specific parameter. For each axis, the individual value for each sample is normalized as a value between the maximum and minimum encountered for that parameter within the dataset. Code used to create the DOM CW can be found at used at https://github.com/paukes/DOM-Comp-Wheel.

Results

DOM concentration & composition

DOM concentrations ranged from 0.1 to 273 mg C/L, with highest mean values in boreal subsurface, pond, and creek samples (Fig 2; S1 File). Highest DOM concentrations were found in subsurface environments in Yellowknife, while the lowest concentrations were found in high arctic environments (Fig 2). High arctic seeps, rivers, and lakes also generally had the lowest average DOC:DON values, but higher average specific ultra-violet absorbance at 255 nm (SUVA), spectral slope ($S_{275-295}$), and HSF values than other locations. SUVA and spectral slope values covered the known range as described broadly in the literature (SUVA: 1.1 to 21 L/(mg·m); spectral slope: 0.005 to 0.032 nm^{-1}). Highest SUVA values (>11 L/(mg·m)) were found at the bottom of a boreal lake and in the high arctic subsurface, but absorbance may be affected by high iron concentrations [14,21]. These two sites were not included further in the discussion. Values of DOC:DON ranged between 9 to 124, and were lowest in rivers and high

arctic samples. Humic substances fraction (HSF) ranged from 14% to 85% and on average were lowest in lakes. Overall, subsurface samples contained the highest DOC:DON and HSF values, and lowest $S_{275-295}$. Hence, both DOM concentration and composition varied across geographic scales and hydrological environments.

PCA on DOM composition measures

The first three principal component axes explained 66% of the variance in DOM composition using the measures contained in the dataset, with PC1 and PC2 accounting for 54% of the variability (Fig 3). Comparison of the first two principal components (PC) yield four distinct groupings of strongly-contributing measures: I) SUVA, SAC_{420}, SAC_{350}; II) HSF, HS MW; III) $S_{275-295}$, E_2:E_3, and S_R; and IV) BB, LMWN, and BP. Groups I and II were negatively associated to groups III and IV. Highest contributions to PC1 and PC2 axes were HSF, SAC_{350}, SAC_{420}, SUVA, and $S_{275-295}$. Variables with contribution to PC1 and PC2 lower than 2% were E_4:E_6, DOC:DON, $S_{350-400}$, and LMWA (Fig. S1). Absorbance parameters normalized to DOM concentrations (SAC_{350}, SAC_{420}, and SUVA) all plotted closely to each other and trended positively with measures of HSF, HSF molecular weight, and DOC:DON. Absorbance techniques plotted perpendicular to LC-OCD size fractions (Fig 3).

Based on contribution to the first two PC axes, we selected four DOM composition measures to define DOM composition. Further, these selected measures are quasi-independent as they are based on different analytical principles or attributes (SUVA, $S_{275-295}$: two different absorbance aspects; HSF: size-exclusion chromatography; DOC:DON: stoichiometry). Although the absorbance at different wavelengths within a sample are closely related [23], they can be used to provide different information on DOM components as one characterizes the amount of UV-absorbing components normalized to DOM concentration at a specific

wavelength (SUVA) while the other is associated with the shape of the absorbance spectra and varies with the distribution of DOM molecular weights ($S_{275-295}$). These four measures include three high-contributing variables to PC1 and PC2 axes (HSF, SUVA, and $S_{275-295}$). The length of the CW axis, and thus CW size, is dictated by the range of each compositional measure encountered in the entire dataset. Composition Wheels are then used as a basis for comparing DOM.

Composition Wheel Shapes

Different environments are characterized by different shapes. Ponds and lakes tend to have lower values of SUVA and DOC:DON and higher $S_{275-295}$, resulting in a triangle shape elongated to the top-right corner (Fig 4). Subsurface DOM samples form a trapezoidal shape due to higher HSF and SUVA values than other sites. Differences in shape are found within locations between different hydrologic settings whereas similarities in shape are found within hydrological setting across locations. For instance, Yellowknife pond sites are similar in shape to subsurface DOM, while the creek, lake, and river shapes reflect DOM with higher $S_{275-295}$, lower DOC:DON, and lower HSF. Representation of different measures using these shapes allows for a facile comparison of DOM composition among samples.

Shapes also help to visualize and highlight the most extremes in DOM composition for each location. The spread of compositions is not evenly distributed between such extreme shapes at any given site but sampling was not targeted *a priori* based on shape. Most surface water sites contained a range in DOM composition between these extremes, forming either shapes similar to subsurface DOM or thin, elongated triangles in the $S_{275-295}$ direction. For this reason, extremes were highlighted in sites with many different shapes to help identify a continuum of possible DOM sources or mixtures (Fig 4). Further, some sites did not conform to

these end-members, as seen by the ELA creek sample with high DOC:DON, allowing easy identification of anomalous data or sites that may warrant further investigation.

Discussion

Comparison of DOM composition measures

Ranges in individual measures of DOM composition are large at both low and high concentrations of DOM (Fig 4, S2 Table) making it difficult to consistently separate sites or hydrological environments across different measures. For instance, accounting for both DOM concentration and DOC:DON may help differentiate some locations, but the range in DOC:DON values across moderate DOM concentrations covers most sites (Fig 2). Hence, new techniques that simultaneously consider different aspects of DOM composition, and are independent of concentration, are needed to compare variations in DOM composition across sample types and environments.

Different characterization techniques provide different information on DOM. In particular, the perpendicular relationship between absorbing and non-absorbing parameters observed among the first two PC axes indicate a range in different DOM properties are captured. For instance, all ELA creeks contain high and similar HSF values, yet we can use absorbance techniques based on molecular weight or UV-absorbing capability (via SUVA; Fig 2) to differentiate between these samples. However, correlations between size-based and absorbance parameters do not mean causation. For example, higher SUVA values are not consistently related to HSF proportions as often assumed. Daring Lake creeks have high SUVA but low HSF. Although absorbance parameters are easily measured and helpful in comparing different

DOM compositions, they do not accurately reflect non-absorbing components (e.g. stoichiometry or functional groups) that could differ among samples.

Associations between independent measures also provide a better understanding of DOM properties that have environmentally-relevant implications. DOM with a high UV-absorbing capacity (high SUVA value) when associated with larger molecular weight components (lower $S_{275\text{-}295}$ and higher HSF values; Fig 3) have implications for heat budgets and stratification within lakes [39]. Lower molecular weight components, as described by $S_{275\text{-}295}$, plot similarly in the PCA to higher proportions of degraded HSF such as BB [40], and, in some instances, can help to identify DOM exposed to sunlight [15]. The similar direction of both HSF and DOC:DON PCA vectors indicate that larger, humic-like molecules within DOM likely contain the minority of nitrogen moieties (Fig 3), also observed among Swedish lakes [41] and northern German streams [42]. Associations between characterization techniques (as quantified, for example by PCA) not only help to determine measures most useful to describe DOM composition, but also avoid overlap of information from related measures that provide similar information.

Effects of DOM Processes and CW End Members

Similar DOM CW shapes were found within hydrologic settings even though samples were collected from sites with varying climates and vegetation, spanning areas of boreal shield watersheds (IISD-ELA) to the high xeric arctic with relatively productive wetlands (Lake Hazen). Further, the range in values across the four CW measures compared well with DOM from other studies (i.e. similar DOM concentrations and SUVA values to rivers in the United States [16,38] and Canadian boreal lakes [43]) indicating that DOM composition and CW shape may not be unique to its locale. The similarity in CW shapes across different locations may result from analogous drivers of DOM fate. For instance, the proportion of biodegradable DOM

was found to be a function of DOM composition and nutrients, rather than ecosystem or region-specific characteristics [44], suggesting that differences in the quality of DOM may not result from location alone. Molecular moieties that persist within the environment can be common across different sites, as observed in a 120-lake survey of boreal lakes in Sweden where 95% of all unique molecular DOM compounds within the dataset could be identified from only 45 lakes [25]. Hence, CWs can be used to amalgamate different compositional measures and quantify similarities in DOM sources and processing across a range of geomorphic, climate, and vegetation environments.

Composition Wheels can be further used to determine the degree of DOM degradation and facilitate comparisons of change along the aquatic continuum. This requires knowledge of the effect of processing, as well as the end-members (e.g. original sources of DOM). Microbial degradation of DOM induces a shift towards higher SUVA and lower DOC:DON (Fig 5; Aukes et al. *in prep.*) but not $S_{275\text{-}295}$, resulting in a distinctive effect of microbial DOM transformation on the CW. Photolytic processing of DOM results in an increase in $S_{275\text{-}295}$ values and a general decrease in the other three DOM quality measures. Further, photolytic degradation affects all four compositional axes, whereas microbial degradation only affects two axes (Fig 5), indicating that certain measures of DOM composition respond differently to different DOM degradation processes. This has important implications for studies using single-characterization techniques as some parameters may not always faithfully serve as useful surrogates for others. For instance, microbial degradation changes SUVA but not HSF (Fig 5), even though SUVA has been linked to DOM aromaticity in humic substances [14]. Thus, comparative differences in a CW can help determine the dominant processes that produce the observed DOM composition of a sample. Although the quantitative response of DOM sources to photo- or microbial degradation is not yet

sufficiently known across different environments, in areas where these rates of change to individual measures have been measured, CWs can be used in a quantitative manner to assess the extent and major processes contributing to DOM loss.

Two dominant DOM compositional end-member shapes are evident in our dataset: subsurface DOM sources and DOM altered by photolysis. Other shapes are intermediate between these two distinctive end-members. High HSF and SUVA in subsurface DOM produce a large trapezoid shape, in contrast to the 'kite-like' shape produced by photolysis (Fig 4). Subsurface DOM CWs are similar across all sites (Fig 4), supporting previous groundwater studies that attribute a narrow DOM compositional range to subsurface processing [45]. Photolysis end-members, identified in a sample by being a similar shape to the final photolysis experiment results (Fig 5), are clearly seen in surface waters and are ubiquitous across all sites (Fig 4). These end-member shapes help constrain the possible range in CW shapes that can be found within aquatic environments.

The subsurface/photolysis end-member categorization frames our conceptual model (Fig 6) that quantifies how the two end-member CW shapes evolve depending on the aquatic-terrestrial hydrologic connection (Fig 6; pathway A-b) or exposure to sunlight (Fig 6: pathway A-B). For instance, creeks with little to no processing of subsurface-derived DOM can be identified by CW shapes similar to subsurface DOM, as seen in ELA and some Daring creeks (Fig 4). ELA lakes have a wide gradient of CW shape and thus overall DOM quality (Fig 4). The use of CW to pair process-based knowledge of DOM composition with hydrologic transport provides a framework that can be used identify key knowledge gaps (i.e. rates of degradation, kinetics based on

composition, water residence time) and quantify the relationship between DOM sources and degree of processing within the environment.

Certain creeks and rivers from YK or WK do not fit into the end-member categories as they contain shapes with larger right sides (higher $S_{275\text{-}295}$ and SUVA than other samples), indicating other processes may be important in determining DOM composition. This may be a result of our sampling of mostly oligotrophic systems that are dominated by terrestrial carbon. We hypothesize that these different shapes represent surface water systems with greater *in-situ*, or autochthonous, contributions of DOM, generally characterized by higher amounts of proteins and smaller molecular weight components [46–48]. Thus, although the dataset was not all comprehensive in terms of the full range of DOM sources, the CW-informed conceptual model provides a framework to build the factors leading to a specific DOM composition.

Adaptability of DOM Composition Wheels

Expressing DOM composition with only four concentration-independent parameters excludes advantages of other techniques not used in this study. However, agreement between multiple parameters allows for selection of surrogates for the CW. LC-OCD is not as widely available but many studies have traditionally used resins [16,49,50] or other size-exclusion columns [51,52] to characterize DOM. Further, LC-OCD fractions of humics have been well correlated to measures of ^{13}C-NMR and fluorescence measures such as HIX [12,42,53]. Although fluorescence was not used in this study, strong associations between certain fluorescence parameters and absorbance or molecular-weight groupings could be used to replace LC-OCD defined fractions, such as using PARAFAC modelling to discern components most similar to HSF [12,42] (Fig 7). These fluorescence parameters are also independent measures of DOM composition and could be readily substituted into the CW. Elemental ratios of DOC:DON

are generally positively correlated with humic-like fluorescence and negatively correlated to protein-like components [41]. Other absorbance indices such as slope ratio and E_2:E_3 (Table 1) are potential surrogates for $S_{275\text{-}295}$ (Fig 2). Measurements of SUVA could be substituted with SAC_{420}, SAC_{350}, or E_4:E_6 [24,41]. However, although SUVA has been correlated with HIX and to fluorescence component C3 [24,41], the opposite has also been found [42]. Associations between different characterization techniques allow for mixing of techniques and comparison of different variables, indicating a wide-range of applicability of CW within environmental sciences.

Clear communication of science and its relevance to society is increasing in importance for both informing the general public and supporting evidence-based policy decisions. The CW visualization method provides an efficient communication tool not only among scientists, but also between scientists and other stakeholders concerned with water quality, including community members. Shapes from CWs show clearly how DOM differs, whereas changes in the numerical value of multiple metrics are only easily grasped by those with familiarity with the methods and environmental ranges. Further work could include pairing different shapes of DOM with key DOM roles such as disinfection demand and by-product formation, metal mobility, and mercury bioaccumulation. By reducing the complexity of independent DOM measures and creating an easily comparable shape, differences in DOM composition can be easily grasped and communicated to larger audiences.

Acknowledgements

We thank Michael English, Roy Judas, and Jordan Reid for field assistance in collecting samples in the Northwest Territories; Paul Dainard, Kyra St. Pierre, Igor Lehnherr, Vince St. Louis, Jessica Serbu, Maria Cavacao, Victoria Wisniewski, and Michael English for field assistance at

Lake Hazen, NU; Will Robertson for assistance at Long Point, ON; Environmental Geochemistry Lab, University of Waterloo for sampling the Grand River, ON; John Spoelstra for sampling Black Brook Watershed, Nottawasaga River Watershed, and Turkey Lakes Watershed. We also thank the Community of Wekweètì and the Wek'èezhìi Land & Water Board for their support, and the Community-Based Monitoring Program and Department of Environment and Natural Resources, Government of Northwest Territories, for collection of samples from the Mackenzie River, NT. We would like thank Richard J. Elgood for logistical, field, and technical help, and Monica Tudorancea assistance with the LC-OCD analysis. We are grateful for the high arctic logistic support provided by Parks Canada, and funding from the Polar Continental Shelf Program (PCSP), Northwest Territories Cumulative Impact Monitoring Program, Northern Scientific Training Program, and the National Science and Engineering Research Council of Canada. PJKA also benefitted from scholarships from the Garfield Weston Foundation, TD Friends of the Environment, and the University of Waterloo. Data used in this manuscript can be found in the publicly-available Wilfrid Laurier University Scholars Portal Dataverse (*doi pending, WLU Scholars Portal Dataverse https://doi.org/10.5683/SP2/NG6D02*), while code used to create the Composition Wheel is available from the corresponding author and https://github.com/paukes/DOM-Comp-Wheel .

References

1. Strock KE, Theodore N, Gawley WG, Ellsworth AC, Saros JE. Increasing dissolved organic carbon concentrations in northern boreal lakes: Implications for lake water transparency and thermal structure. J Geophys Res Biogeosciences. 2017;122: 1022–1035. doi:10.1002/2017JG003767
2. Baken S, Degryse F, Verheyen L, Merckx R, Smolders E. Metal complexation properties of freshwater dissolved organic matter are explained by its aromaticity and by anthropogenic ligands. Environ Sci Technol. 2011;45: 2584–2590. doi:10.1021/es103532a
3. Bauer M, Heitmann T, Macalady DL, Blodau C. Electron transfer capacities and reaction kinetics of peat dissolved organic matter. Environ Sci Technol. 2007;41: 139–145.

doi:10.1021/es061323j

4. Matilainen A, Gjessing ET, Lahtinen T, Hed L, Bhatnagar A, Sillanpää M. An overview of the methods used in the characterisation of natural organic matter (NOM) in relation to drinking water treatment. Chemosphere. 2011;83: 1431–1442. doi:10.1016/j.chemosphere.2011.01.018

5. Krasner SW, Weinberg HS, Richardson SD, Pastor SJ, Chinn R, Sclimenti MJ, et al. Occurrence of a New Generation of Disinfection Byproducts. Environ Sci Technol. 2006;40: 7175–7185. doi:10.1021/es060353j

6. Evans CD, Monteith DT, Cooper DM. Long-term increases in surface water dissolved organic carbon: observations, possible causes and environmental impacts. Environ Pollut. 2005;137: 55–71. doi:10.1016/j.envpol.2004.12.031

7. Weyhenmeyer GA, Prairie YT, Tranvik LJ. Browning of boreal freshwaters coupled to carbon-iron interactions along the aquatic continuum. PLoS One. 2014;9: e88104. doi:10.1371/journal.pone.0088104

8. Worrall F, Burt TP. Changes in DOC treatability: Indications of compositional changes in DOC trends. J Hydrol. 2009;366: 1–8. doi:10.1016/j.jhydrol.2008.11.044

9. Ritson JP, Graham NJD, Templeton MR, Clark JM, Gough R, Freeman C. The impact of climate change on the treatability of dissolved organic matter (DOM) in upland water supplies: A UK perspective. Sci Total Environ. 2014;473–474: 714–730. doi:10.1016/j.scitotenv.2013.12.095

10. Creed IF, Bergström AK, Trick CG, Grimm NB, Hessen DO, Karlsson J, et al. Global change-driven effects on dissolved organic matter composition: Implications for food webs of northern lakes. Glob Chang Biol. 2018;24: 3692–3714. doi:10.1111/gcb.14129

11. Larsen LG, Aiken GR, Harvey JW, Noe GB, Crimaldi JP. Using fluorescence spectroscopy to trace seasonal DOM dynamics, disturbance effects, and hydrologic transport in the Florida Everglades. J Geophys Res. 2010;115: 1–14. doi:10.1029/2009JG001140

12. Hutchins RHS, Aukes PJK, Schiff SL, Dittmar T, Prairie YT, del Giorgio PA. The Optical, Chemical, and Molecular Dissolved Organic Matter Succession Along a Boreal Soil-Stream-River Continuum. J Geophys Res Biogeosciences. 2017;122: 2892–2908. doi:10.1002/2017JG004094

13. Kellerman AM, Guillemette F, Podgorski DC, Aiken GR, Butler KD, Spencer RGM. Unifying Concepts Linking Dissolved Organic Matter Composition to Persistence in Aquatic Ecosystems. Environ Sci Technol. 2018;52: 2538–2548. doi:10.1021/acs.est.7b05513

14. Weishaar JL, Aiken GR, Bergamaschi BA, Fram MS, Fujii R, Mopper K. Evaluation of specific ultraviolet absorbance as an indicator of the chemical composition and reactivity of dissolved organic carbon. Environ Sci Technol. 2003;37: 4702–4708. doi:10.1021/es030360x

15. Helms JR, Stubbins A, Ritchie JD, Minor EC, Kieber DJ, Mopper K. Absorption spectral slopes and slope ratios as indicators of molecular weight, source, and photobleaching of chromophoric dissolved organic matter. Limnol Oceanogr. 2008;53: 955–969. doi:10.4319/lo.2008.53.3.0955

16. Spencer RGM, Butler KD, Aiken GR. Dissolved organic carbon and chromophoric dissolved organic matter properties of rivers in the USA. J Geophys Res Biogeosciences. 2012;117. doi:10.1029/2011JG001928

17. Stedmon C a, Markager S, Bro R. Tracing dissolved organic matter in aquatic environments using a new approach to fluorescence spectroscopy. Mar Chem. 2003;82: 239–254. doi:10.1016/S0304-4203(03)00072-0
18. Jaffé R, Yamashita Y, Maie N, Cooper WT, Dittmar T, Dodds WK, et al. Dissolved Organic Matter in Headwater Streams: Compositional Variability across Climatic Regions of North America. Geochim Cosmochim Acta. 2012;94: 95–108. doi:10.1016/j.gca.2012.06.031
19. Hunt AP, Parry JD, Hamilton-Taylor J. Further evidence of elemental composition as an indicator of the bioavailability of humic substances to bacteria. Limnol Oceanogr. 2000;45: 237–241.
20. Huber SA, Balz A, Abert M, Pronk W. Characterisation of aquatic humic and non-humic matter with size-exclusion chromatography – organic carbon detection – organic nitrogen detection (LC-OCD-OND). Water Res. 2011;45: 879–885. doi:10.1016/j.watres.2010.09.023
21. Poulin B a, Ryan JN, Aiken GR. Effects of Iron on Optical Properties of Dissolved Organic Matter. Environ Sci Technol. 2014; 1–20. doi:10.1021/es502670r
22. Mead J. The Control of Fe and pH on the Photodegradation and Characterization of Dissolved Organic Matter in Small, Oligotrophic Canadian Shield Freshwaters. University of Waterloo. 2017.
23. Massicotte P, Asmala E, Stedmon C, Markager S. Global distribution of dissolved organic matter along the aquatic continuum: Across rivers, lakes and oceans. Sci Total Environ. 2017;609: 180–191. doi:10.1016/j.scitotenv.2017.07.076
24. Kellerman AM, Kothawala DN, Dittmar T, Tranvik LJ. Persistence of dissolved organic matter in lakes related to its molecular characteristics. Nat Geosci. 2015;8. doi:10.1038/ngeo2440
25. Kellerman AM, Dittmar T, Kothawala DN, Tranvik LJ. Chemodiversity of dissolved organic matter in lakes driven by climate and hydrology. Nat Commun. 2014;5: 1–8. doi:10.1038/ncomms4804
26. Creed IF, Mcknight DM, Pellerin BA, Green MB, Bergamaschi BA, Aiken GR, et al. The river as a chemostat : fresh perspectives on dissolved organic matter flowing down the river continuum. Can J Fish Aquat Sci. 2015;14: 1–14.
27. Hur J, Park M-H, Schlautman MA. Microbial transformation of dissolved leaf litter organic matter and its effects on selected organic matter operational descriptors. Environ Sci Technol. 2009;43: 2315–21. doi:10.1021/es802773b
28. Hansen AM, Kraus TEC, Pellerin BA, Fleck JA, Downing BD, Bergamaschi BA. Optical properties of dissolved organic matter (DOM): Effects of biological and photolytic degradation. Limnol Oceanogr. 2016;61: 1015–1032. doi:10.1002/lno.10270
29. Koehler B, Von Wachenfeldt E, Kothawala DN, Tranvik LJ. Reactivity continuum of dissolved organic carbon decomposition in lake water. J Geophys Res Biogeosciences. 2012;117: 1–14. doi:10.1029/2011JG001793
30. Koehler B, Tranvik LJ. Reactivity continuum modeling of leaf, root, and wood decomposition across biomes. J Geophys Res G Biogeosciences. 2015;120: 1196–1214. doi:10.1002/2015JG002908
31. Catalán N, Casas-Ruiz JP, von Schiller D, Proia L, Obrador B, Zwirnmann E, et al. Biodegradation kinetics of dissolved organic matter chromatographic fractions in an intermittent river. J Geophys Res Biogeosciences. 2017;122: 131–144.

doi:10.1002/2016JG003512
32. Lundin EJ, Klaminder J, Bastviken D, Olid C, Hansson S V., Karlsson J. Large difference in carbon emission - Burial balances between boreal and arctic lakes. Sci Rep. 2015;5: 1–7. doi:10.1038/srep14248
33. Marshall IB, Schut PH, Ballard M. A National Ecological Framework for Canada: Attribute Data [Internet]. Ottawa, ON, Canada: Ecosystem Stratification Working Group, Agriculture and Agri-Food Canada & Environment Canada; 1999. Available: http://sis.agr.gc.ca/cansis/nsdb/ecostrat/1999report/index.html
34. Dahlén J, Bertilsson S, Pettersson C. Effects of UV-A radiation on dissolved organic matter in humic surface waters. Environ Int. 1996;22: 501–506.
35. Chin Y-P, Aiken GR, O'Loughlin E. Molecular Weight, Polydispersity, and Spectroscopic Properties of Aquatic Humic Substances. Environ Sci Technol. 1994;28: 1853–1858. doi:10.1021/es00060a015
36. Curtis PJ, Schindler DW. Hydrologic control of dissolved organic matter in low-order Precambrian Shield lakes. Biogeochemistry. 1997;36: 125–138. doi:10.1023/A:1005787913638
37. R Core Team. R: A language and environment for statistical computing. [Internet]. Vienna, Austria: R Foundation for Statistical Computing; 2020. Available: http://www.r-project.org
38. Jaffé R, McKnight D, Maie N, Cory RM, McDowell WH, Campbell JL. Spatial and temporal variations in DOM composition in ecosystems: The importance of long-term monitoring of optical properties. J Geophys Res. 2008;113: 1–15. doi:10.1029/2008JG000683
39. Pilla RM, Williamson CE, Zhang J, Smyth RL, Lenters JD, Brentrup JA, et al. Browning-Related Decreases in Water Transparency Lead to Long-Term Increases in Surface Water Temperature and Thermal Stratification in Two Small Lakes. J Geophys Res Biogeosciences. 2018;123: 1651–1665. doi:10.1029/2017JG004321
40. Tercero Espinoza LA, ter Haseborg E, Weber M, Frimmel FH. Investigation of the photocatalytic degradation of brown water natural organic matter by size exclusion chromatography. Appl Catal B Environ. 2009;87: 56–62. doi:10.1016/j.apcatb.2008.08.013
41. Kothawala DN, Stedmon CA, Müller RA, Weyhenmeyer GA, Köhler SJ, Tranvik LJ. Controls of dissolved organic matter quality: Evidence from a large-scale boreal lake survey. Glob Chang Biol. 2014;20: 1101–1114. doi:10.1111/gcb.12488
42. Bodmer P, Heinz M, Pusch M, Singer GA, Premke K. Carbon dynamics and their link to dissolved organic matter quality across contrasting stream ecosystems. Sci Total Environ. 2016;553: 574–586. doi:10.1016/j.scitotenv.2016.02.095
43. Mueller KK, Fortin C, Campbell PGC. Spatial Variation in the Optical Properties of Dissolved Organic Matter (DOM) in Lakes on the Canadian Precambrian Shield and Links to Watershed Characteristics. Aquat Geochemistry. 2012;18: 21–44. doi:10.1007/s10498-011-9147-y
44. Lapierre J-F, del Giorgio PA. Partial coupling and differential regulation of biologically and photochemically labile dissolved organic carbon across boreal aquatic networks. Biogeosciences. 2014;11: 5969–5985. doi:10.5194/bg-11-5969-2014
45. Shen Y, Chapelle FH, Strom EW, Benner R. Origins and bioavailability of dissolved organic matter in groundwater. Biogeochemistry. 2015;122: 61–78. doi:10.1007/s10533-

014-0029-4

46. Tank SE, Lesack LFW, Gareis J a. L, Osburn CL, Hesslein RH. Multiple tracers demonstrate distinct sources of dissolved organic matter to lakes of the Mackenzie Delta, western Canadian Arctic. Limnol Oceanogr. 2011;56: 1297–1309. doi:10.4319/lo.2011.56.4.1297
47. Roiha T, Peura S, Cusson M, Rautio M. Allochthonous carbon is a major regulator to bacterial growth and community composition in subarctic freshwaters. Sci Rep. 2016;6: 34456. doi:10.1038/srep34456
48. Hood E, Fellman JB, Spencer RGM, Hernes PJ, Edwards R, D'Amore D V., et al. Glaciers as a source of ancient and labile organic matter to the marine environment. Nature. 2009;462: 1044–7. doi:10.1038/nature08580
49. Cleveland CC, Neff JC, Townsend AR, Hood E. Composition, Dynamics, and Fate of Leached Dissolved Organic Matter in Terrestrial Ecosystems: Results from a Decomposition Experiment. Ecosystems. 2004;7: 275–285. doi:10.1007/s10021-003-0236-7
50. Bourbonniere R. Distribution patterns of dissolved organic matter fractions in natural waters from eastern Canada. Org Geochem. 1989;14: 97–107. doi:10.1016/0146-6380(89)90023-5
51. Her N, Amy GL, Foss D, Cho J, Yoon Y, Kosenka P. Optimization of method for detecting and characterizing NOM by HPLC-size exclusion chromatography with UV and on-line DOC detection. Environ Sci Technol. 2002;36: 1069–76. Available: http://www.ncbi.nlm.nih.gov/pubmed/11917993
52. Kawasaki N, Matsushige K, Komatsu K, Kohzu A, Nara FW, Ogishi F, et al. Fast and precise method for HPLC-size exclusion chromatography with UV and TOC (NDIR) detection: importance of multiple detectors to evaluate the characteristics of dissolved organic matter. Water Res. 2011;45: 6240–6248. doi:10.1016/j.watres.2011.09.021
53. Romera-Castillo C, Chen M, Yamashita Y, Jaffé R. Fluorescence characteristics of size-fractionated dissolved organic matter: Implications for a molecular assembly based structure? Water Res. 2014;55C: 40–51. doi:10.1016/j.watres.2014.02.017

Tables

Table 1. Dissolved organic matter composition as described by chemical, absorbance, and molecular-size based measures used in this study.

Measure (*common abbreviation*)	Equation	Unit	Characteristic	Reference
Chemical				
DOC:DON	$M_C \div M_N$	-	Stoichiometry	[19]
Absorbance				
E_2:E_3	$A_{255} \div A_{365}$	-	Inversely related to molecular size	[34]
E_4:E_6	$A_{465} \div A_{665}$	-	Humic molecular weight and size	[35]
SAC_{350}	$\frac{ln(10) \times A_{420}/L}{[\mathrm{DOC}]}$	$\frac{\mathrm{cm}^2}{\mathrm{mg\text{-}C}} \div 10^3$	Specific absorbance at 350 nm and attributed to colour	[36]
SAC_{420}	$\frac{ln(10) \times A_{420}/L}{[\mathrm{DOC}]}$	$\frac{\mathrm{L}}{\mathrm{mg} \times \mathrm{m}}$	Specific absorbance at 420 nm	
SUVA	$\frac{ln(10) \times A_{255}/L}{[\mathrm{DOC}]}$	$\frac{\mathrm{L}}{\mathrm{mg} \times \mathrm{m}}$	Correlated to degree of aromaticity	[14]
$S_{275\text{-}295}$	$a_\lambda = a_{\lambda_{275}} e^{-S(\lambda-275)}$	nm^{-1}	Inversely related to MW (where *S* is the slope)	[15]
$S_{350\text{-}400}$	$a_\lambda = a_{\lambda_{350}} e^{-S(\lambda-350)}$	nm^{-1}	Used with $S_{275\text{-}295}$ to calculated S_R	[15]
S_R	$\frac{S_{275-295}}{S_{350-400}}$	-	Inversely related to overall molecular weight; integrative indicator of light-absorbing DOM history	[15]
Size Exclusion Chromatography				
Biopolymers (BP)	-	% of DOM	Polysaccharides, proteins	[20]
Humic substances (HSF)	-	% of DOM	Humic or fulvic-like components	[20]
Building Blocks (BB)	-	% of DOM	Degraded HS	[20]
Low-molecular weight neutrals (LMWN)	-	% of DOM	Aldehydes, small organic materials	[20]
Low-molecular weight acids (LMWA)	-	% of DOM	Saturated mono-protic acids	[20]
HS molecular weight (HS MW)	-	g / mol	Nominal average molecular weight of HS	[20]

Figures

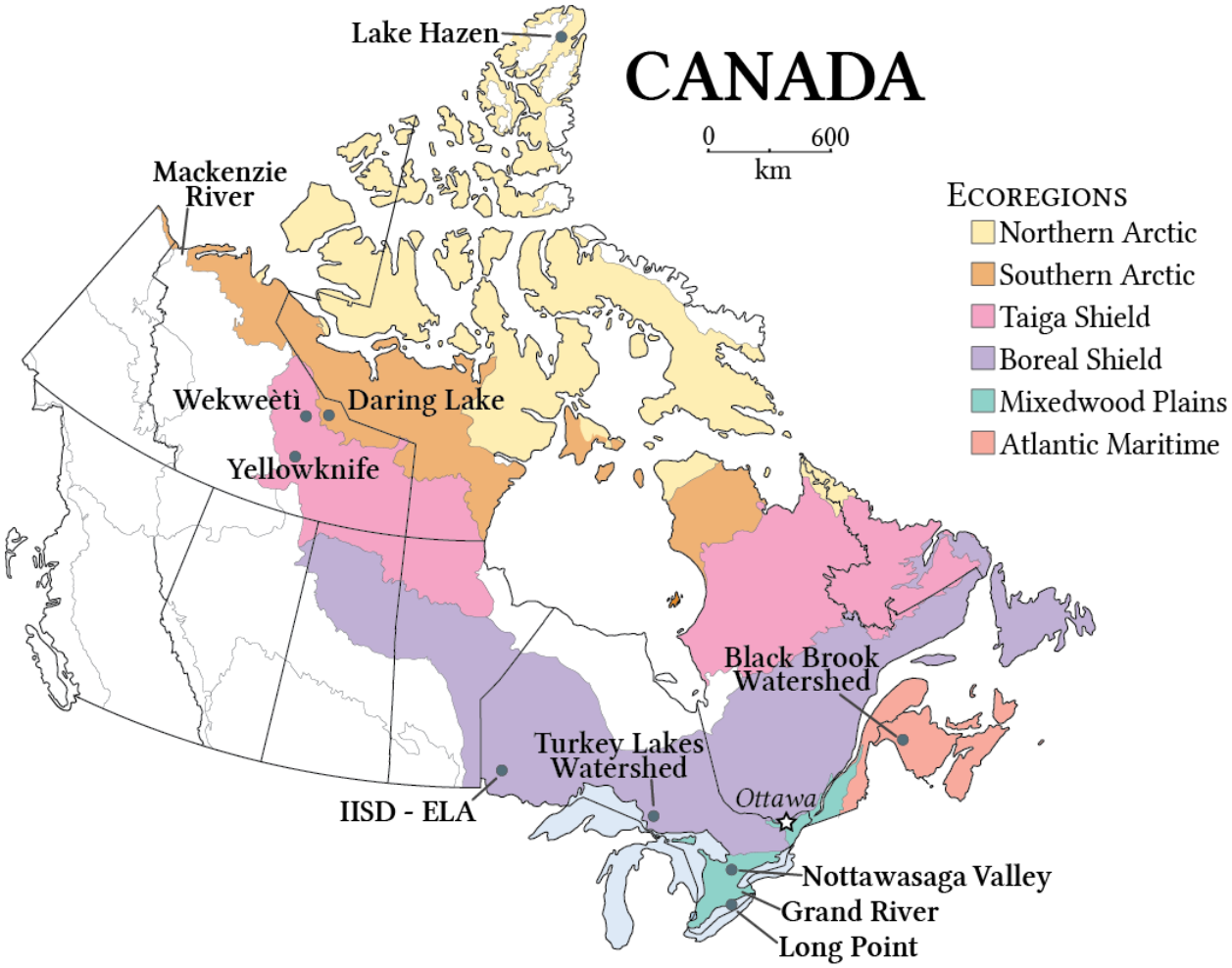

Fig 1. Locations of sampling sites and ecozones. River locations (Grand River, ON; Mackenzie River, NT) are labelled at the mouth of the river.

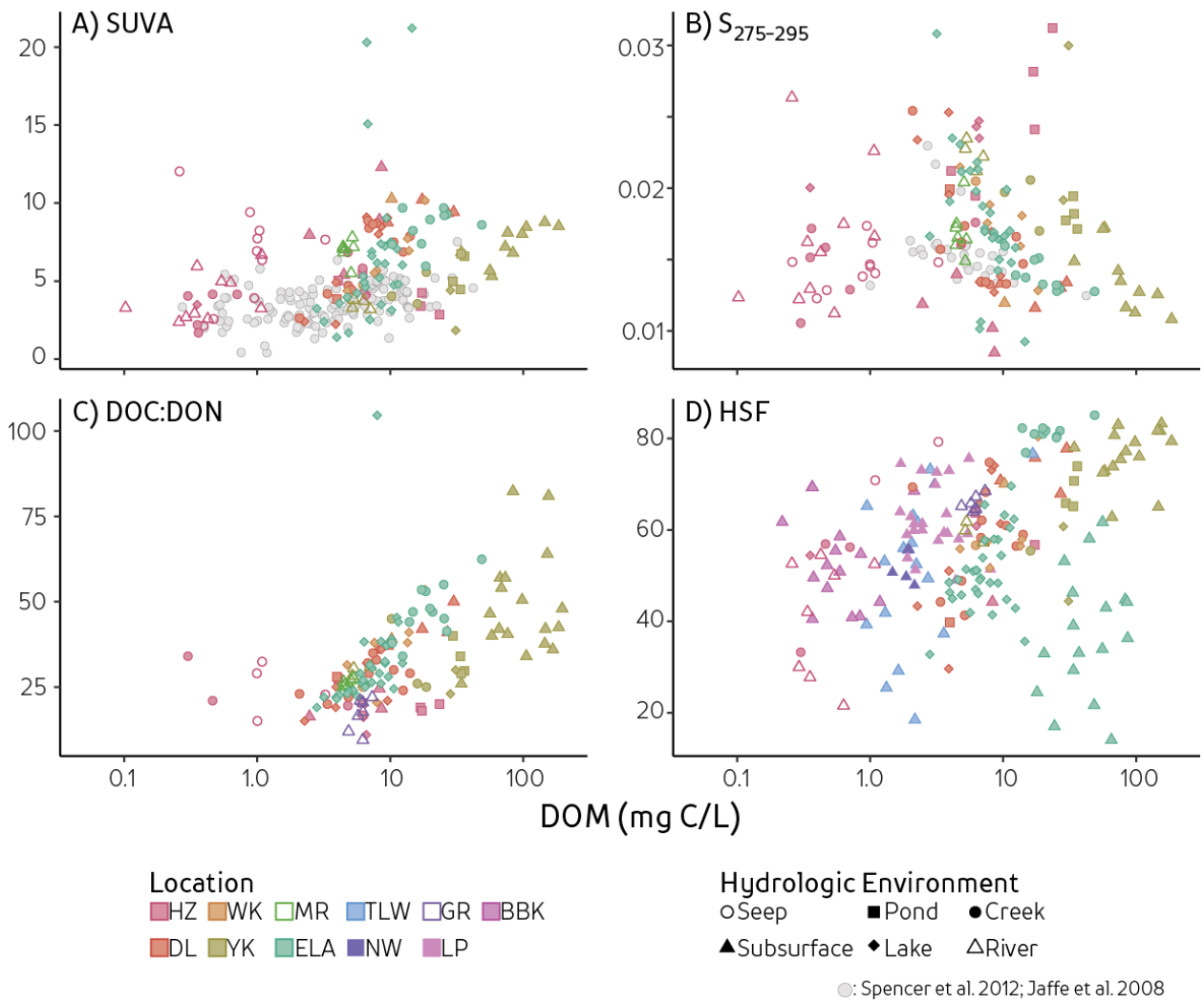

Fig 2. Compositional measures versus total DOM concentration. Measures include A) SUVA, specific ultraviolet absorbance at 255 nm, B) $S_{275\text{-}295}$, spectral slope between 275 to 295nm, C) DOC:DON, and D) HSF; humic substances fraction. Colours represent geographical sampling locations (HZ: Lake Hazen Watershed, NU; DL: Daring Lake, NT; WK: Wekweètì, NT; YK: Yellowknife, NT; MR: Mackenzie River, NT; ELA: IISD-Experimental Lakes Area, ON; TLW: Turkey Lakes Watershed, ON; NW: Nottawasaga River Watershed, ON; GR: Grand River, ON; LP: Long Point, ON; BBK: Black Brook Watershed, ON) while shapes represent hydrologic environments. Light grey circles represent two other published DOM characterization studies conducted at similar scales [16,38].

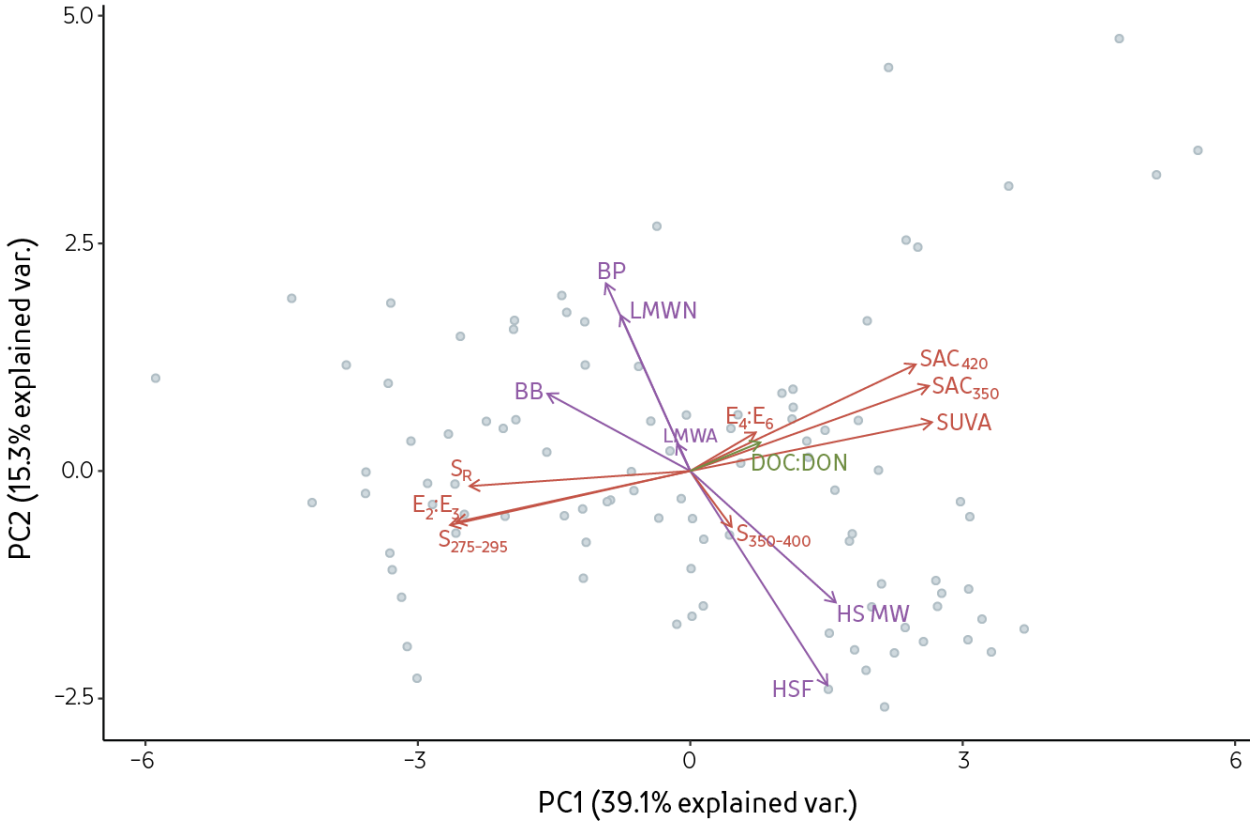

Fig 3. Principal component analyses for samples from different ecozones. Grey dots represent individual samples, while vectors represent absorbance (red), elemental (green), and LC-OCD (purple) compositional measures.

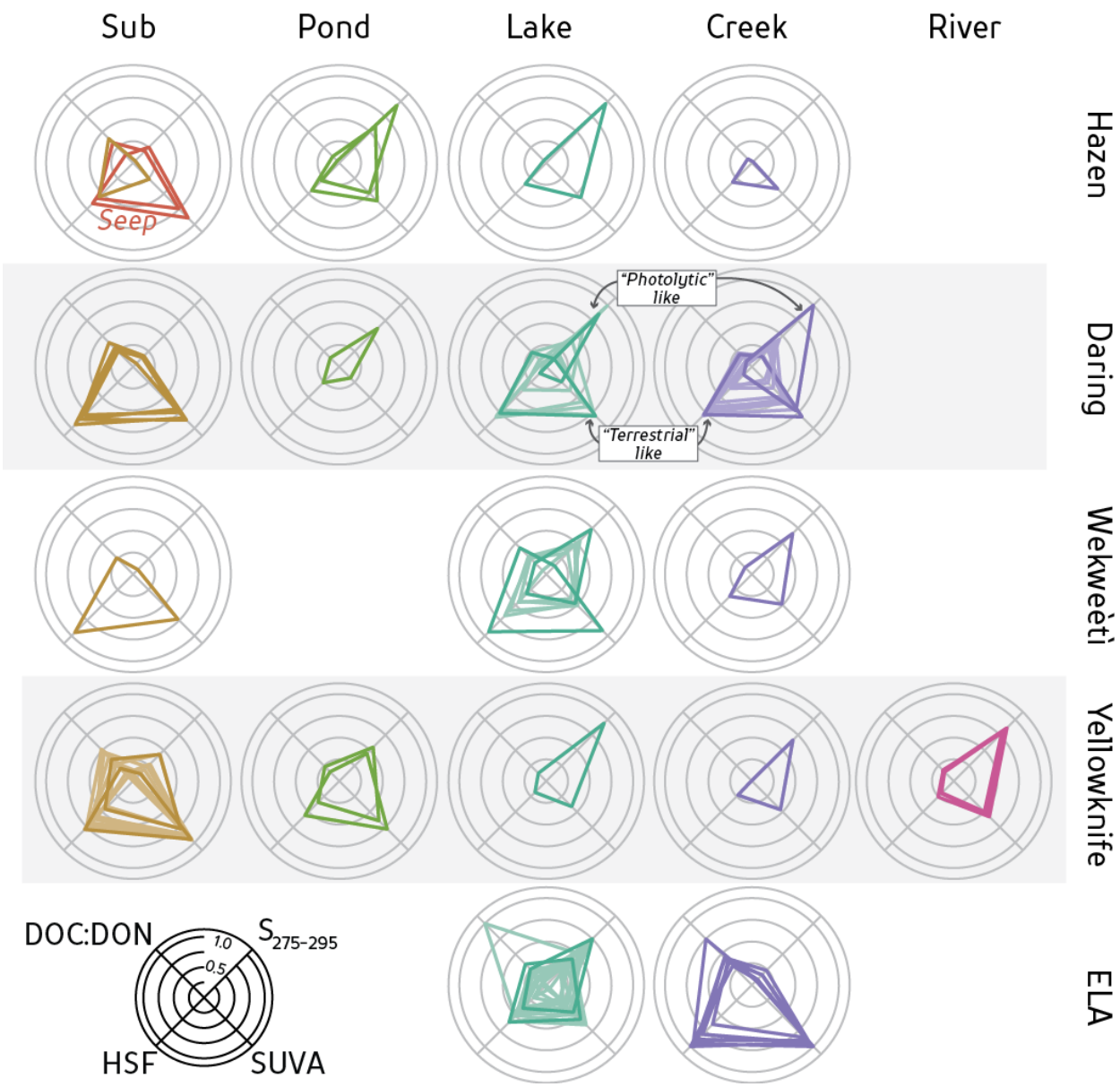

Fig 4. Composition wheels for DOM from different hydrologic settings within each geographical site. Axes are a numerical value normalized relative to the maximum and minimum encountered within the dataset for each parameter. Parameters for each axis found in bottom left. The orientation of the composition wheel (CW) axes are arbitrary. Different samples from the same hydrological and geographic setting are plotted within the same CW. Two 'end member' compositions are highlighted in sites with many samples to help visualize the continuum of DOM mixtures: subsurface-like DOM (low DOC:DON, high SUVA and HSF) or photolyzed DOM (high $S_{275\text{-}295}$).

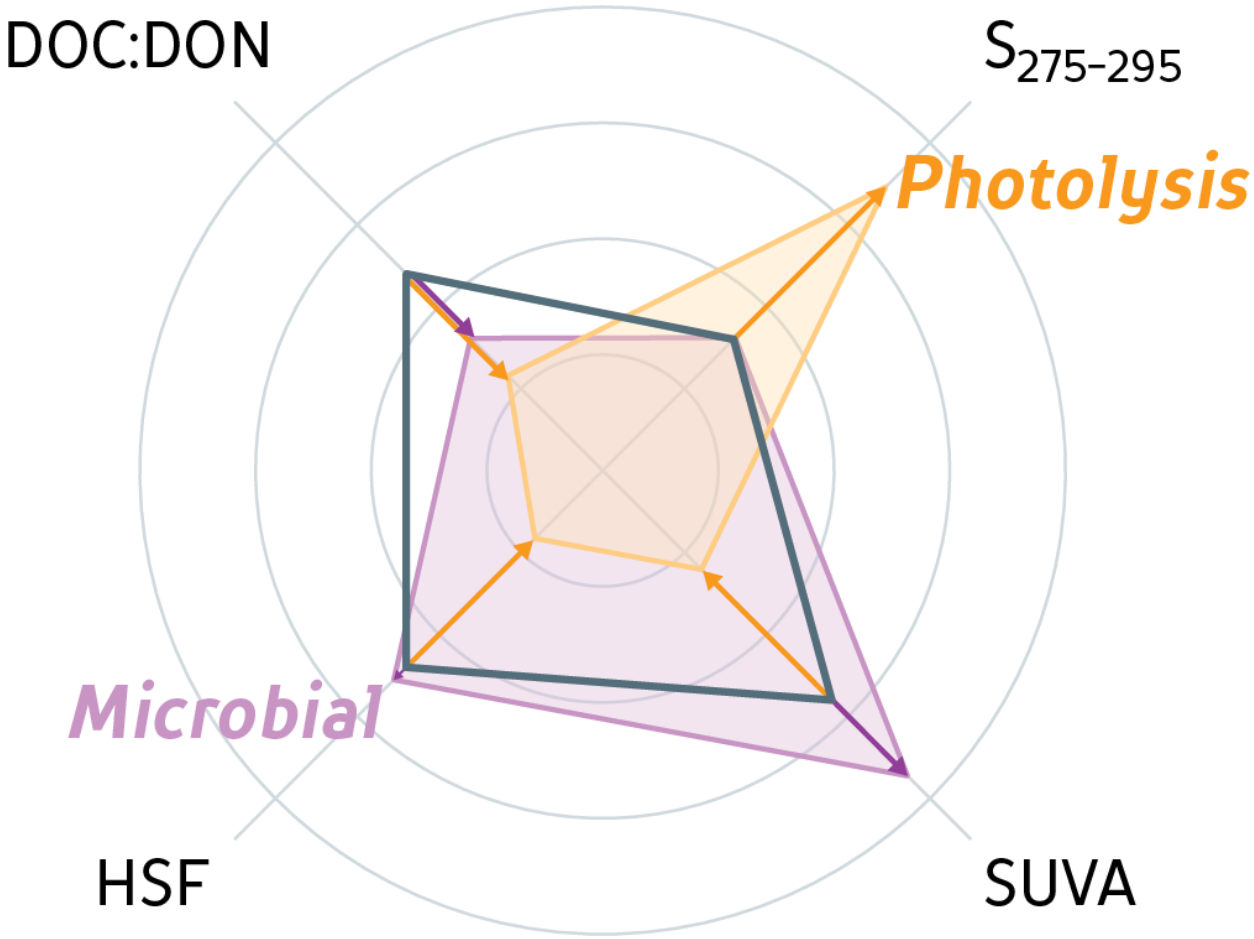

Fig 5. Changes to a Composition Wheel resulting from photolytic and microbial degradation. Changes to dissolved organic matter (DOM) (grey) with photolytic (orange; 12 to 18 day exposure to sunlight) or microbial (purple; 30-day experiment) degradation based on experimental incubations of natural DOM samples (Aukes et al. *in prep*) and analysis of samples typical of subsurface and surface water environments. The mean decrease in DOM concentration was 18% during photolysis and 10% during microbial degradation experiments (n=11, 9; respectively).

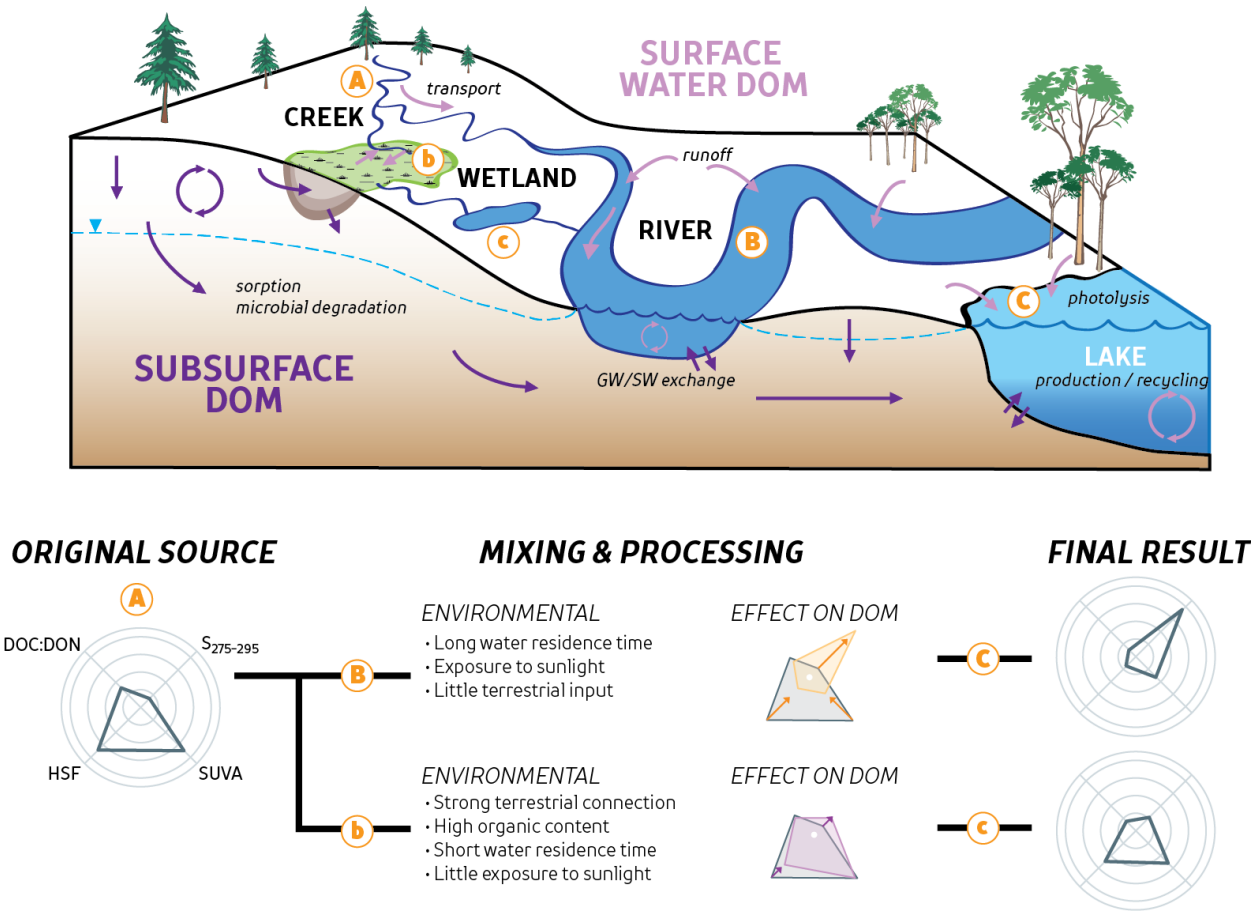

Fig 6. Conceptual model of DOM evolution along the aquatic continuum. A conceptual model of select processes and sources of dissolved organic matter (DOM) along the aquatic continuum. Arrows represent the transport or addition of DOM among subsurface (dark purple) and surface waters (light purple), while lowercase text highlights some of the specific processes and sources encountered. The use of Composition Wheels to illustrate differences in sources and processing is shown on the bottom panel, comparing DOM from an organic-rich source with longer exposure to sunlight (A, B, C) versus the same DOM with less sunlight exposure and greater microbial degradation (A, b, c).

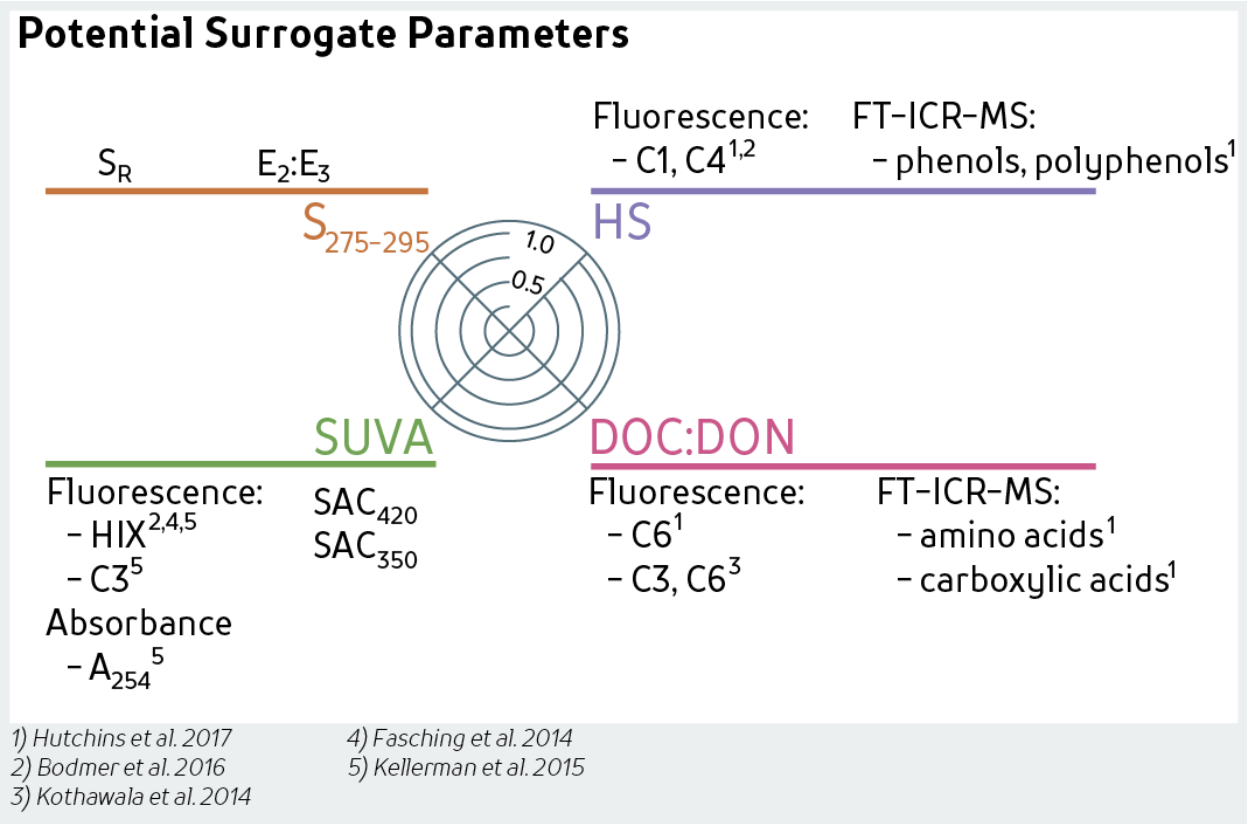

Fig 7. Surrogate parameters for the DOM Composition Wheel.

Supporting information

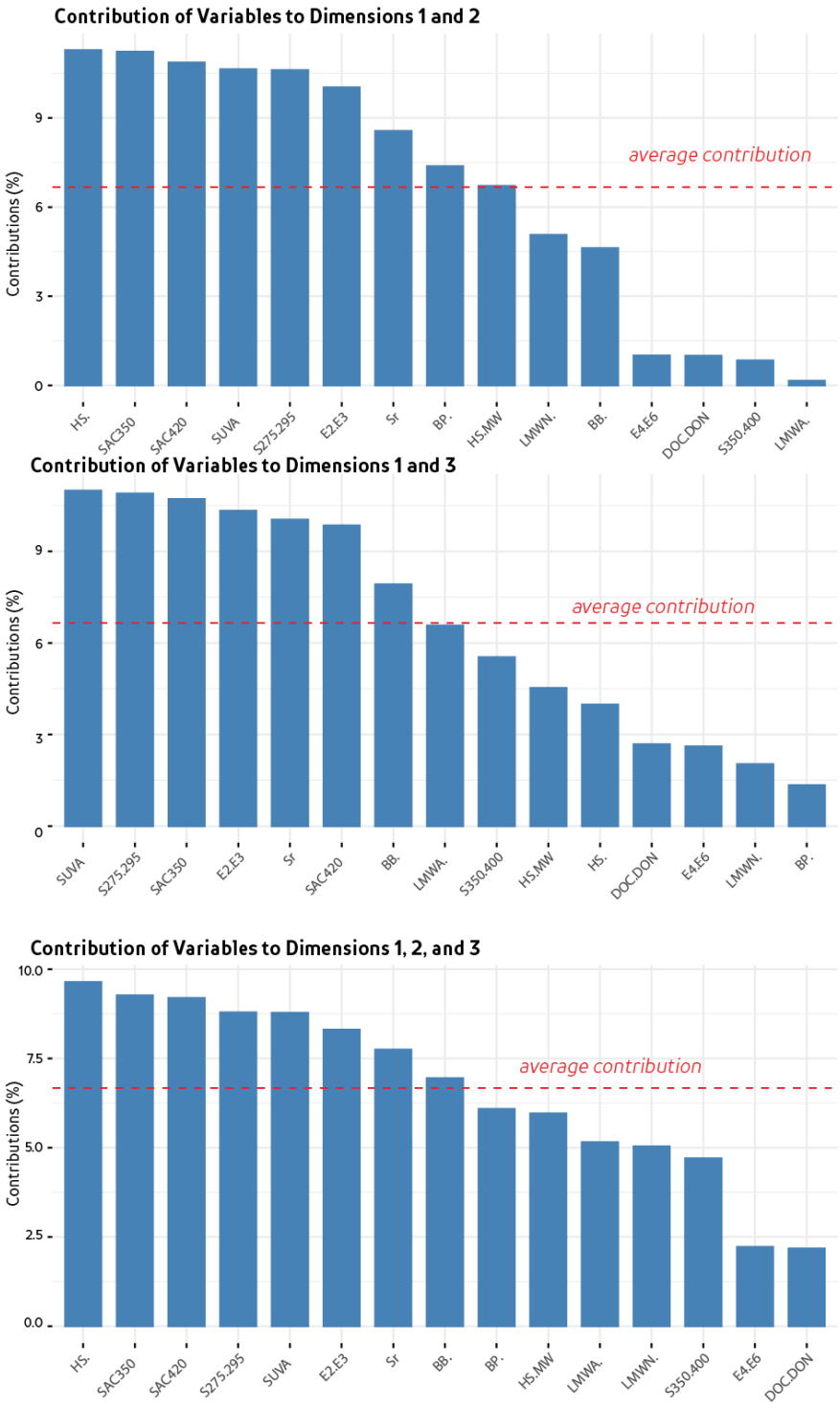

S1 Fig. Contribution of each variable within the PCA.

S1 Table. Environmental description for all sampling sites. Included are the number of total samples taken for DOM concentration with at least one compositional measure (n_{DOC}), and number of samples used from that site in the PCA analysis (n_{PCA}).

SURFACE WATERS				
Name	**Location**	**n_{DOC}**	**n_{PCA}**	**Description**
IISD-Experimental Lakes Area, ON (ELA)	49° 39' 40"N, 93° 43' 48"W Ontario, Canada	**74**	**45**	Boreal forest, underlain by Precambrian bedrock with discontinuous surficial layer of sandy-gravel till. Sampled from 2010 to 2012. Ecozone mean annual temperature: 0.7 C; Ecozone total annual precipitation: 825 mm.
Lakes		*49*	*36*	
Creeks		*25*	*9*	
Grand River, ON (GR)	43° 30' 41"N, 80° 29' 43"W Ontario, Canada	**39**	**-**	Surrounding land predominately agricultural and flows past six wastewater treatment plants. Sampled from 6 consecutive locations along a 90km stretch every two months from 2011 to 2012. Ecozone mean annual temperature: 6.5 C; Ecozone total annual precipitation: 940 mm.
Yellowknife, NT (YK)	62° 27' 14"N, 114° 22' 18"W Northwest Territories, Canada	**23**	**20**	Samples from the Taiga Shield underlain by discontinuous permafrost. Surface waters are surrounded by bedrock and peat plateaux around Yellowknife. Sampled in July or October between 2013 and 2017. Ecozone mean annual temperature: -4.8 C; Ecozone total annual precipitation: 565 mm.
Lakes		*2*	*2*	
Ponds		*8*	*7*	
Rivers		*10*	*9*	
Creek		*3*	*2*	
Mackenzie River, NT (MK)	63° 14' 17"N, 123° 34' 0"W Northwest Territories, Canada	**13**	**-**	Samples taken by the Community Based Monitoring network along the Mackenzie River in July and August of 2015. Samples ranged from WHERE to Inuvik. River flows through Taiga Shield and Taiga Plains.
Rivers		*13*	-	
Wekweètì, NT (WK)	64° 11' 24"N, 114° 11' 10"W Northwest Territories, Canada	**11**	**11**	Situated in the Taiga Shield, below treeline, continuous permafrost. Samples taken in Octber of 2015 and 2016. Ecozone mean annual temperature: -4.8 C; Ecozone total annual precipitation: 565 mm.
Lakes		*9*	*9*	
Creeks		*2*	*2*	
Daring Lake, NT (DL)	64° 31' 29"N, 111° 40' 24"W Northwest Territories, Canada	**19**	**19**	Found in the Southern Arctic above treeline, continuous permafrost. Ecozone mean annual temperature: -9.8 C; Ecozone total annual precipitation: 313 mm.
Lakes		*7*	*7*	
Ponds		*1*	*1*	
Creeks		*11*	*11*	
Lake Hazen, NU (LH)	81° 49' 30"N, 71° 19' 26"W Nunavut, Canada	**160**	**12**	Tundra located in the high arctic; Lake Hazen Watershed is considered a local polar oasis.
Lakes		*38*	*2*	
Ponds		*18*	*4*	
Creeks		*41*	*1*	
Rivers		*32*	*0*	
Seeps		*31*	*5*	

GROUND WATERS				
Name	**Location**	**n**	**nPCA**	**Description**
Turkey Lakes Watershed, ON (TLW)	47° 2' 54"N, 84° 24' 25"W Ontario, Canada	**16**	**-**	Relatively un-impacted watershed in the Great Lakes-St. Lawrence forest region. Area consists of Precambrian bedrock and surficial glacial deposits of glaciofluvial outwash. Samples collected from depths ranging between 0.90 -

				6.89m below surface. Ecozone mean annual temperature: 0.7 C; Ecozone total annual precipitation: 825 mm.
IISD-Experimental Lakes Area, ON (ELA)	49° 39’ 40”N, 93° 43’ 48”W Ontario, Canada	**17**	**-**	Piezometers constructed in transect along a wetland, ranging from 0.70 - 3.85m below surface. Ecozone mean annual temperature: 0.7 C; Ecozone total annual precipitation: 825 mm.
Nottawasaga Aquifer, ON (NW)	44° 7’ 26”N, 79° 49’ 12”W Ontario, Canada	**6**	**-**	Surficial deposits of glaciolacustrine deposits in an agriculturally-impacted aquifer. Samples collected from single multi-level piezometer within an unconfined surficial sand aquifer at depths of 4.35m, 5.13m, 6.68m, 9.90m, and 11.3m below surface. Ecozone mean annual temperature: 6.5 C; Ecozone total annual precipitation: 940 mm.
Black Brook Watershed, NB (BBK)	47° 6’ 11”N, 67° 45’ 40”W New Brunswick, Canada	**15**	**-**	Site is an agriculturally-impacted aquifer, sampled during the summer of 2012. Surficial deposits of till and small deposits of glacial outwash. Samples taken from twelve domestic wells and three multi-level piezometers (6.1 - 30m below surface). Ecozone mean annual temperature: 4.6 C; Ecozone total annual precipitation: 1185 mm.
Long Point, ON (LP)	42° 34’ 46”N, 80° 22’ 57”W Ontario, Canada	**23**	**-**	Unconfined sand aquifer atop of a clay aquitard. Piezometers range from 1 to 4m below surface. Sampling of groundwater containing a septic plume.
Yellowknife, NT (YK)	62° 27’ 14”N, 114° 22’ 18”W Northwest Territories, Canada	**33**	**16**	Samples from the Taiga Shield underlain by discontinuous permafrost. Surface waters are surrounded by bedrock and peat pleataux around Yellowknife. Sampled in July or October between 2013 and 2017. Ecozone total annual precipitation: 565 mm.
Wekweètì, NT (WK)	64° 11’ 24”N, 114° 11’ 10”W Northwest Territories, Canada	**1**	**1**	Situated in the Taiga Shield, below treeline, continuous permafrost. Samples taken in October of 2015 and 2016. Ecozone total annual precipitation: 565 mm.
Daring Lake, NT (DL)	64° 31’ 29”N, 111° 40’ 24”W Northwest Territories, Canada	**4**	**4**	Found in the Southern Arctic above treeline, continuous permafrost. Ecozone mean annual temperature: -9.8 C; Ecozone total annual precipitation: 313 mm.
Lake Hazen, NU (LH)	81° 49’ 30”N, 71° 19’ 26”W Nunavut, Canada	**17**	**2**	Samples taken from piezometer installed at deepest extent of active-layer (~0.25m). Location was in a subcatchment containing organic-rich soil. Flow direction was through wetland into nearby lake. Organic-rich layer underlain by silt or clay material.

S2 Table. DOM Composition versus Concentration Statistics. Results from a linear model of dissolved organic matter (DOM) composition (SUVA, slope between 275-295nm, DOC:DON,

and humic substances fraction) as predicted by the overall DOM concentration (mg C/L; log transformed).

Parameter	**Linear Regression to log(DOM)**	
	R^2	p-value
SUVA	0.10	<0.01
S275	0.01	0.61
DOC:DON	0.33	<0.01
HSF	0.09	<0.01